G_2-QCD: Spectroscopy and the phase diagram at zero temperature and finite density

Bjoern H. Wellegehausen[*]
Justus-Liebig-University Giessen and Friedrich-Schiller-University Jena
E-mail: bjoern.wellegehausen@theo.physik.uni-giessen.de

Lorenz von Smekal
Justus-Liebig-University Giessen and TU Darmstadt
E-mail: lorenz.smekal@physik.tu-darmstadt.de

Axel Maas and Andreas Wipf
Friedrich-Schiller-University Jena
E-mail: axelmaas@web.de, wipf@tpi.uni-jena.de

Due to the fermion sign problem, standard lattice Monte-Carlo method for QCD fail at small temperatures and high baryon densities. G_2-QCD, QCD with the gauge group $SU(3)$ replaced by the exceptional Lie group G_2, can be simulated using lattice techniques at these densities, and can therefore provide an illustration of the possible phase structure. Here we present a systematic investigation of the ground-state hadronic spectrum using lattice simulations for different quark masses in several hadronic sectors. We then show that the different hadronic scales of Goldstone bosons, intermediate bosons, and baryons is reflected in the phase structure at finite density.

---

[*]Speaker.

1. Introduction

QCD at finite baryon density suffers from a severe sign problem and its phase diagram can therefore not be treated with standard Monte-Carlo methods [1]. Several approaches to QCD have been investigated to circumvent this problem, but so far all these approaches failed to describe the phase diagram at high baryon density and small temperature. A different strategy is to investigate QCD-like theories, as for instance 2-color QCD [2, 3], to gain insight into gauge theories at finite density. However, these theories should share as much features as possible with QCD. Here we replace the gauge group $SU(3)$ by the exceptional Lie group G_2. G_2-QCD is a gauge theory with fermionic baryons and fundamental quarks [4, 5] and it can be simulated without sign problem at finite density and temperature. In the present article we discuss the theoretical foundations of (lattice) spectroscopy for G_2-QCD and present our results for the vacuum spectrum of states and the phase diagram at zero temperature obtained from lattice simulations on a rather small $8^3 \times 16$ lattice. We find that we can observe structures at finite density at scales which correspond to scales we find in the hadronic spectrum. Especially, we find onsets of transitions at scales corresponding to the Goldstone scale, the intermediate boson scale, and the baryonic scale. The results indeed suggest that the theory has a rich phase structure, and that baryonic-dominated regions of the phase diagram may exist.

2. Chiral symmemtry and baryon number in G_2-QCD

The Euclidean action of N_f flavour G_2-QCD with baryon chemical potential μ reads

$$S = \int d^4 x \, \text{tr} \left\{ -\frac{1}{4} F_{\mu\nu} F^{\mu\nu} + \sum_{n=1}^{N_\text{f}} \bar{\Psi}_n D[A, m, \mu] \Psi_n \right\} \quad \text{with}$$

$$D[A, m, \mu] = \gamma_\text{E}^{\mu} (\partial_\mu - g A_\mu) - m + \gamma_{\text{E}_0} \mu, \tag{2.1}$$

where the gauge group is the exceptional Lie group G_2. The fundamental representations of G_2 are 7-dimensional and 14-dimensional, the latter coinciding with the adjoint representation. The elements of G_2 can be viewed as elements of $SO(7)$ subject to seven independent cubic constraints for the 7-dimensional matrices g representing $SO(7)$ [4],

$$T_{abc} = T_{def} \, g_{da} \, g_{eb} \, g_{fc}, \tag{2.2}$$

where T is a total antisymmetric tensor. Since G_2 is a subgroup of $SO(7)$, all representations are real. The Dirac operator satisfies

$$D(\mu)^\dagger \gamma_5 = \gamma_5 D(-\mu^*) \quad \text{and} \quad D(\mu)^* T = T D(\mu^*) \tag{2.3}$$

with $T = C\gamma_5$, $T^* T = -\mathbb{1}$, $T^\dagger = T^{-1}$ and charge conjugation matrix C. If such a unitary operator T exists then the eigenvalues of the Dirac operator come in complex conjugate pairs, all real eigenvalues are doubly degenerate [2, 6] and thus

$$\det D[A, m, \mu] \geq 0 \quad \text{for} \quad \mu \in \mathbb{R}. \tag{2.4}$$
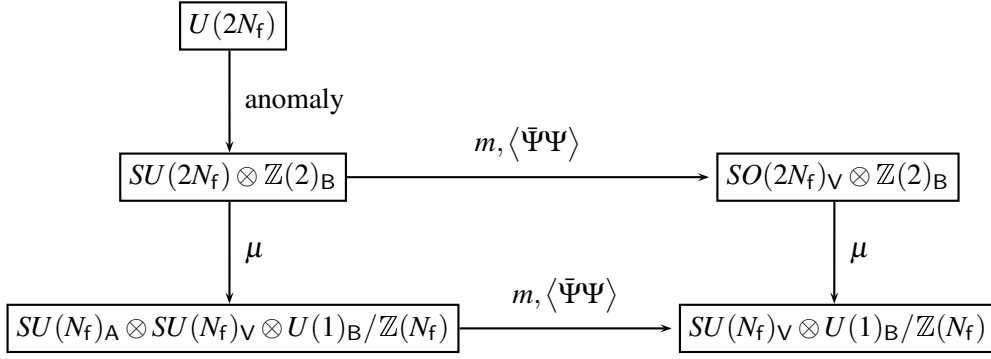
Figure 1: Pattern of chiral symmetry breaking in G_2-QCD.

Since the gauge field A_μ is real and anti-symmetric, it is possible to write the matter part of the action (2.1) for $\mu = 0$ as a sum over $2N_f$ Majorana spinors λ_n

$$\mathscr{L}[\Psi, A] = \bar{\Psi} D[A, m, 0] \Psi = \bar{\lambda} D[A, m, 0] \lambda \tag{2.5}$$

with $\lambda = (\chi, \eta) = (\lambda_1, \dots, \lambda_{2N_f})$. It follows that G_2-QCD possesses an extended flavour symmetry [2] compared to QCD. The action is invariant under the $SO(2N_f)_V$ vector transformations $\lambda \mapsto e^{\beta \otimes \mathbb{1}} \lambda$ with a real and antisymmetric $\beta \in \mathfrak{so}(2N_f)$ and the axial transformations $\lambda \mapsto e^{i\alpha \otimes \gamma_5} \lambda$ with a real symmetric matrix α. Due to the Majorana constraint left- and right-handed spinors cannot be rotated independently and the general transformation is a composition of axial- and vector transformations, leading to a $U(2N_f)$ symmetry group, in agreement with the results in [4]. Following the same arguments as in QCD it is expected that the axial $U(1)$ is broken by the axial anomaly such that only a $SU(2N_f) \times \mathbb{Z}(2)_B$ chiral symmetry remains. In the presence of a non-vanishing Dirac mass term (or a non-vanishing chiral condensate) the theory is no longer invariant under the axial transformations. Therefore the non-anomalous chiral symmetry is expected to be broken explicitly (or spontaneously) to its maximal vector subgroup,

$$SU(2N_f) \otimes \mathbb{Z}(2)_B \mapsto SO(2N_f)_V \otimes \mathbb{Z}(2)_B, \tag{2.6}$$

Since baryon chemical potential is an off-diagonal term in Majorana flavour space, the remaining chiral symmetry at finite baryon chemical potential is the same as in QCD,

$$SU(2N_f) \otimes \mathbb{Z}(2)_B \mapsto SU(N_f)_A \otimes SU(N_f)_V \otimes U(1)_B / \mathbb{Z}(N_f). \tag{2.7}$$

The final pattern of chiral symmetry breaking of G_2-QCD is shown in figure 1. If chiral symmetry is spontaneously broken, the axial chiral multiplet becomes massless, according to the Goldstone theorem. In contrast to QCD, because of the enlarged chiral symmetry group, already in the case of a single Dirac flavour a non-trivial chiral symmetry is present, and chiral symmetry breaking can be observed. In this $N_f = 1$ case chiral symmetry is given by $SU(2) \otimes \mathbb{Z}(2)_B$ leading to two Goldstone bosons

$$d(0^{++}) = \bar{\Psi}^C \gamma_5 \Psi - \bar{\Psi} \gamma_5 \Psi^C \quad \text{and} \quad d(0^{+-}) = \bar{\Psi}^C \gamma_5 \Psi + \bar{\Psi} \gamma_5 \Psi^C. \tag{2.8}$$

with baryon number $n_B = 2$[1]. They are scalar diquarks instead of pseudoscalar mesons as in QCD.

---

[1]In our definition baryon number counts the difference of quarks and anti-quarks

3. Spectroscopy for $N_f = 1$ G_2-QCD

Since the centre of G_2 is trivial, we expect to find bound states with every integer baryon number. Beside the states that are also present in QCD, Mesons with baryon number $n_B = 0$ and nucleons with $n_B = 3$, there are additional states like diquarks with $n_B = 2$ or more exotic bound states of gluons and quarks, for example a hybrid with $n_B = 1$. In the following we give an overview over our implementation of possible bound states for $N_f = 2$ G_2-QCD, see tables 1 and 2. In all tables

Name	$\mathcal{O}$	J	P	C
π	$\bar{u}\gamma_5 d$	0	-	+
η	$\bar{u}\gamma_5 u$	0	-	+
a	$\bar{u}d$	0	+	+
f	$\bar{u}u$	0	+	+
ρ	$\bar{u}\gamma_\mu d$	1	-	+
ω	$\bar{u}\gamma_\mu u$	1	-	+
b	$\bar{u}\gamma_5\gamma_\mu d$	1	+	+
h	$\bar{u}\gamma_5\gamma_\mu u$	1	+	+

Name	$\mathcal{O}$	J	P	C
$d(0^{++})$	$\bar{u}^C\gamma_5 u + c.c.$	0	+	+
$d(0^{+-})$	$\bar{u}^C\gamma_5 u - c.c.$	0	+	-
$d(0^{-+})$	$\bar{u}^C u + c.c.$	0	-	+
$d(0^{--})$	$\bar{u}^C u - c.c.$	0	-	-
$d(1^{++})$	$\bar{u}^C\gamma_\mu d - \bar{d}^C\gamma_\mu u + c.c.$	1	+	+
$d(1^{+-})$	$\bar{u}^C\gamma_\mu d - \bar{d}^C\gamma_\mu u - c.c.$	1	+	-
$d(1^{-+})$	$\bar{u}^C\gamma_5\gamma_\mu d - \bar{d}^C\gamma_5\gamma_\mu u + c.c.$	1	-	+
$d(1^{--})$	$\bar{u}^C\gamma_5\gamma_\mu d - \bar{d}^C\gamma_5\gamma_\mu u - c.c.$	1	-	-

Table 1: Bosonic bound states with baryon number $n_B = 0$ (left table) and $n_B = 2$ (right table).

Name	$\mathcal{O}$	J	P	C
N'	$T^{abc}(\bar{u}_a\gamma_5 d_b)u_c$	1/2	$\pm$	$\pm$
Δ'	$T^{abc}(\bar{u}_a\gamma_\mu u_b)u_c$	3/2	$\pm$	$\pm$
Hybrid	$\varepsilon_{abcdefg}u^a F_{\mu\nu}^{bc}F_{\mu\nu}^{de}F_{\mu\nu}^{fg}$	1/2	$\pm$	$\pm$

Name	$\mathcal{O}$	J	P	C
N	$T^{abc}(\bar{u}_a^C\gamma_5 d_b)u_c$	1/2	$\pm$	$\pm$
Δ	$T^{abc}(\bar{u}_a^C\gamma_\mu u_b)u_c$	3/2	$\pm$	$\pm$

Table 2: Fermionic bound states with baryon number $n_B = 1$ (left table) and $n_B = 3$ (right table).

$\mathcal{O}$ is the interpolating operator used to extract the mass in the lattice simulation and J, P, C the spin, parity and charge conjugation quantum numbers. In our lattice simulations the $N_f = 2$ G_2-QCD states are included by partial quenching, i. e. two valence quark flavor, but only one sea quark flavor. If isospin is unbroken, the masses of flavour singlet diquarks and flavour non-singlet mesons are degenerate. For example the diquark correlation function

$$C_d(x,y) = \left\langle \bar{\chi}(x)\gamma_5\chi(x)\,\bar{\chi}(y)\gamma_5,\chi(y) \right\rangle \tag{3.1}$$

contains only connected contributions. The corresponding correlation function for the η meson reads

$$C_\eta(x,y) = \left\langle \eta(x)\eta^\dagger(y) \right\rangle = 2\left\langle \bar{\chi}(x)\gamma_5\chi(x)\,\bar{\chi}(y)\gamma_5\chi(y) \right\rangle + C_d(x,y) \tag{3.2}$$

where the difference to the diquark correlation function is only the disconnected contribution, showing that the π has the same mass as the $d(0^+)$. Analog relations lead to

$$m_{d(0^+)} = m_{\pi(0^-)}, \quad m_{d(0^-)} = m_{a(0^+)}, \quad m_{d(1^+)} = m_{\rho(1^-)}, \quad m_{d(1^-)} = m_{b(1^+)}. \tag{3.3}$$

Thus, for every diquark there is a flavour non-singlet meson with the same mass but opposite parity.

4. Lattice spectroscopy results

In order to fix our parameters we compute the scalar and vector diquark masses and the proton mass for different parameters of the inverse gauge coupling β and the hopping parameter κ on a $8^3 \times 16$ lattice. The results are shown in figure 2. The mass ratios between the scalar and vector
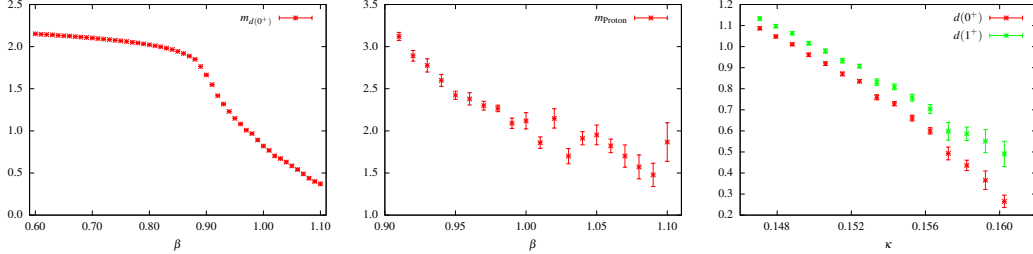

Figure 2: Left panel: Mass of the pseudo Goldstone boson as a function of β for $\kappa = 0.147$. **Center panel:** Mass of the proton as a function of β for $\kappa = 0.147$. **Right panel:** Mass of the 0^+ and the 1^+ diquark as a function of κ for $\beta = 0.96$.

diquarks and between the scalar diquarks and nucleons allow us to estimate the distance from the chiral limit, since they should go to zero in the chiral limit while they approach 1 and 2/3 for heavy quarks. In the following we discuss two different ensembles with parameters shown in table 3.

Ensemble	β	κ	$m_{d(0^+)}a$	$m_N a$	$m_{d(0^+)}$ [MeV]	a [fm]	a^{-1} [MeV]	MC
Heavy	1.05	0.147	0.59(2)	1.70(9)	326	0.357(33)	552(50)	7K
Light	0.96	0.159	0.43(2)	1.63(13)	247	0.343(45)	575(75)	5K

Table 3: Parameters for two different ensembles. All results are from a $8^3 \times 16$ lattice.

Our mass scale is set by the proton mass, $m_N = 938$ MeV. For the heavy quark ensemble (Fig. 3,
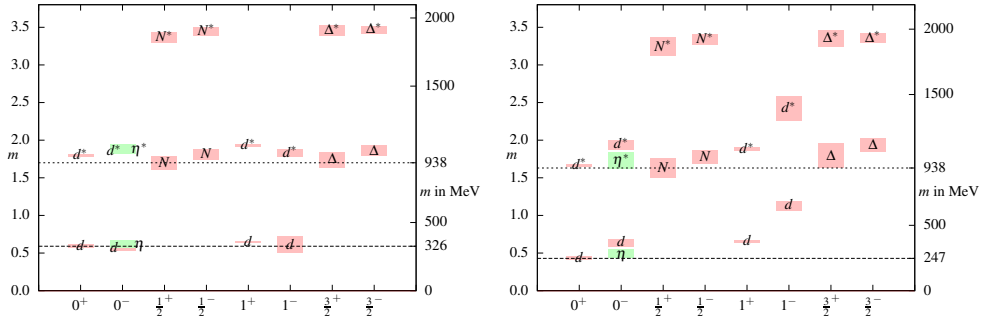

Figure 3: The mass spectrum of the heavy (left panel) and light (right panel) ensemble is shown.

left panel) the diquark masses are almost degenerate and the η has essentially the same mass as the diquarks. For the nucleons there is almost no mass splitting between parity even and odd states. In the light ensemble (Fig. 3, right panel), the diquark masses are no longer degenerate. We observe a significant mass splitting between parity even and odd states as well as between scalar and vector diquarks. Especially, the Goldstone boson becomes the lightest state, with the η also

being somewhat heavier. For the nucleons we also observe different masses for parity even and odd states and the spin 1/2 and spin 3/2 representations. We find three clearly different scales in the light spectrum: A Goldstone scale, an intermediate boson scale set by the remaining diquarks, and the nucleon scale set by the N and Δ.

5. G_2-QCD at zero temperature and finite baryon density

We will now show that the different hadronic scales observed in the spectra in Fig. 3 reflect themselves in the structure of the finite density phase diagram. In figure 4 (left panel) we show the quark number density n_q from vanishing chemical potential up to saturation. We observe that for small
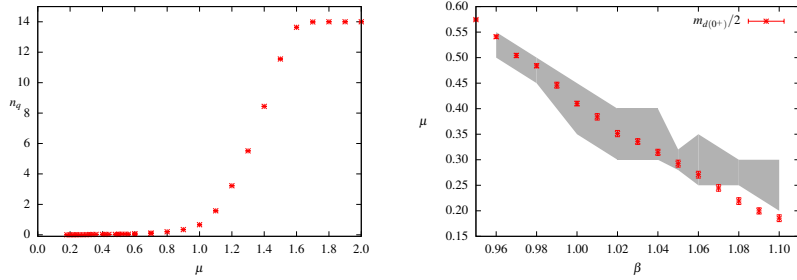
Figure 4: Left panel: The quark number density as a function of chemical potential are shown. **Right panel:** The onset transition observed in the quark number density is compared to half of the mass of the lightest state, the 0^+ diquark, for different gauge couplings β.

values of the chemical potential the system remains in the vacuum, i. e. the quark number density vanishes, which is expected due to the silver blaze property. When increasing the chemical potential further the quark number density starts rising, indicating that baryonic matter is present and the system is no longer in the vacuum state. At even larger values of μ the quark number density saturates, in agreement with the theoretical prediction of $n_{q,\mathrm{max}} = 2N_{\mathrm{c}} = 14$ [5]. A closer look into this phase diagram at zero temperature, see Fig. 4 (right panel), shows the manifestation of the silver blaze property for baryon chemical potential: The quark number density shows an onset transition to a non-vacuum state when chemical potential reaches half of the mass of the lightest baryon, the Goldstone 0^+ diquark. For larger values of chemical potential a series of plateaus develops where the quark number density is almost constant, see figure 5. At around $\mu = 0.6$ for the heavy ensemble and $\mu = 0.55$ for the light ensemble the quark number density starts increasing again and no further plateau is observed. For the heavy ensemble, in addition to the silver blaze transition due to the diquark states we find good agreement of the Δ mass with the point where the quark number density increases without building a plateau. For the light ensemble the two transitions at $\mu \approx 0.22$ and $\mu \approx 0.32$, each followed by a plateau, can be related to the observation of the splitting of the 0^+ and 0^- diquark masses. Again the transition at $\mu \approx 0.55$ is in good agreement with the Δ mass divided by three. For both ensembles our observation is thus that transitions in the quark number density coincide with hadron masses divided by their baryon number. For a bosonic hadron a plateau is formed after the transition while for a fermionic hadron the quark number density increases further with increasing chemical potential. In both ensembles we observe also a transition at $\mu \approx 0.52$ (heavy ensemble) and $\mu \approx 0.38$ (light ensemble) that does not coincide with any of our
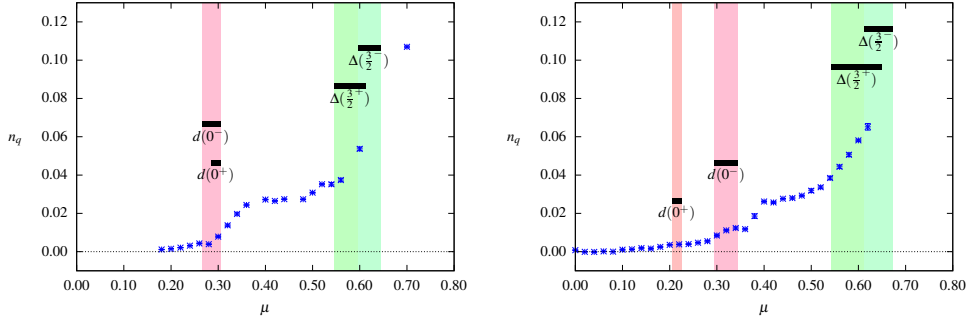
Figure 5: Shown is the quark number density compared to baryon mass divided by baryon number for the heavy ensemble (left panel) and the light ensemble (right panel).

spectroscopic states. Since this transition is followed by a plateau we speculate that this state might be a bosonic hadron. A possible candidate could for example be a bound state of four quarks.

6. Conclusions

On a rather small lattice we have presented the hadronic spectrum of G_2-QCD obtained with lattice Monte-Carlo simulations. For sufficiently small quark masses different hadronic scales related to the Goldstone sector and nucleonic sector develop, quite similar to the situation in ordinary QCD. We have also shown that this scale hierarchy of the vacuum reflects itself in the phase structure at finite densities. The phase diagram at zero temperature shows a number of transitions which correlate with the scales of the hadron spectrum. This already indicates a very rich phase structure of the theory and ongoing investigations aim at a deeper understanding of the phase diagram of G_2-QCD at finite density.

Acknowledgments

References

[1] C. Gattringer and C.B. Lang, Lect.Notes Phys. 788 (2010) 1–343

[2] J.B. Kogut, M.A. Stephanov et al., Nucl.Phys. B 582 (2000) 477–513

[3] S. Hands, P. Kenny, S. Kim and J. Skullerud, Eur.Phys.J. A 47 (2011) 60

[4] K. Holland, P. Minkowski, M. Pepe and U.J. Wiese, Nucl. Phys. B 668 (2003) 207–236

[5] A. Maas, L.v. Smekal, B.H. Wellegehausen and A. Wipf, Phys.Rev. D 86 (2012)

[6] S. Hands, I. Montvay, S. Morrison, M. Oevers and L. Scorzato, Eur.Phys.J. C 17 (2000) 285–302